DESIGN AND VALIDATION OF ADVANCED TRANSONIC WINGS USING CFD AND VERY HIGH REYNOLDS NUMBER WIND TUNNEL TESTING

Mark I. Goldhammer
Boeing Commercial Airplane Group
and
Frank W. Steinle, Jr.
NASA Ames Research Center

Abstract

The aerodynamic technology of transonic commercial transport wings has improved dramatically over the past 40 years. The early-generation wings were based largely on NACA airfoil sections integrated simply into three-dimensional designs. Airfoils with a more peaky pressure distribution characterized the second generation of transports. More recent designs have been developed with a major influence from computational fluid dynamics (CFD) and have relied less on iterative wind tunnel testing.

As the next generation of transports evolves, continuing the trend toward improved aerodynamic technology becomes increasingly difficult as the limiting flow physics are approached. However, competitive pressure within the airframe industry and the need to satisfy the airline operator to reduce costs in a deregulated environment continues to spur the need for further wing advances.

The work summarized here opens the possibility for further wing aerodynamic technology advances when the design and test environment is at a significantly higher Reynolds number than used for previous generations of commercial transports. It is shown that, coupled with advances in CFD modeling of wings and improvements in test techniques, further improvements in wing technology can be developed at significantly higher Reynolds numbers.

I. Introduction

The aerodynamic design process for commercial transport wings has undergone tremendous changes since the first jets were introduced in the 1950s. Not only has the design process changed from a largely empirical approach to a combination of testing and CFD, but also the development time has been reduced and flight characteristics prediction precision requirements have been increased by competitive pressures within the industry.

Considerable progress has been made over the years as shown in figure 1. The first generation of designs were characterized by NACA empirically derived airfoil sections, which were employed in rather simple three-dimensional (3D) wing designs. The second generation, which includes the early widebodies, employed somewhat more advanced airfoils and used early subsonic panel methods for three-dimensional integration. Designs from the last decade made considerable use of advanced airfoil sections usually designed through the use of sophisticated two-dimensional (2D) transonic/viscous CFD methods. Early three-dimensional transonic methods also began to be employed in the development of these designs, primarily small disturbance methods that lacked reliable viscous modeling.

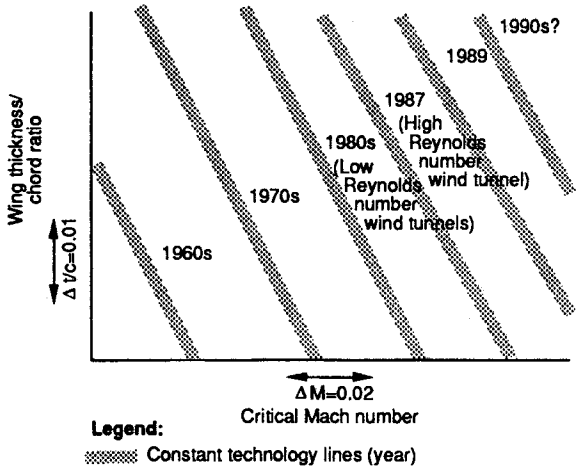

Figure 1. Chronological Improvement in Mach Technology

It is clear from figure 1 that several major advances in wing aerodynamic technology have been achieved. The primary reason for the advances has been in the underlying transonic airfoil technology. It is also shown in figure 1 that further advances were achieved in the latter part of the 1980s, at least in the wind tunnel. These advances are attributable not only to further airfoil technology improvements, but also to improved 3D design and to improved testing technology. Improved viscous modeling, both in CFD formulations and in testing at higher Reynolds numbers, have contributed to this latest technology improvement.

There are two major underlying flow physics that limit the design technology of transonic wings. The first limit is the development of strong shock waves as a consequence of the thickness and lifting requirements of the wing. The second limit, and one that has perhaps been underemphasized earlier, is the viscous limits of the flow.

As 2D and 3D transonic/viscous CFD methods continue to evolve through cycles of concept identification and validation, the wing aerodynamicist has more and more information available from which to base design judgments. Modern designs are concerned with both the shock wave and viscous characteristics of the flow. Off-design considerations, including drag, buffet, and stability characteristics, can be considered more rigorously in the wing design philosophy using CFD. With this added knowledge, validated in high Reynolds number wind tunnel testing, further technology advances can be achieved.

As the viscous part of the design emerges as a flow limit of importance comparable to the shock wave, it has become increasingly important for the wing aerodynamicist to have a realistic test environment. CFD can model the flight scale flows, but validation or calibration of the CFD methods requires substantially higher test Reynolds numbers than has been used previously by industry. In addition, design philosophies of the past were required to be demonstrated at relatively small fractions of the flight Reynolds number, figure 2. Test techniques to provide low Reynolds number simulation of flight conditions, namely a combination of aft transition fixing and free transition testing, were devised. These testing techniques placed limits on the wing design philosophies allowed. Therefore, further technology advances might be demonstrated with increased test Reynolds number.

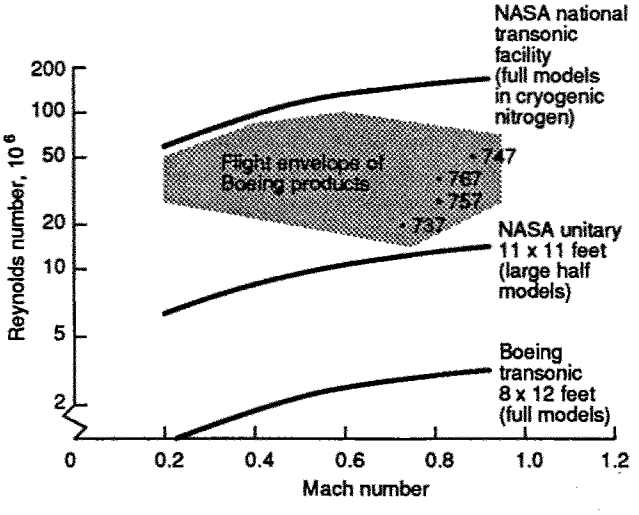

Figure 2. Reynolds Number Spectrum of Wind Tunnels and Commercial Airplanes

The technology of increasing the test Reynolds number to approach the region of interest for large commercial transports is a formidable task. Efforts in the U.S.A. and Europe to develop full-scale test capability using cryogenic nitrogen have progressed considerably; but to date, these facilities do not offer an efficient means of acquiring the large amounts of test data required to commit a new design to production. This paper reports on a study conducted by the Boeing Commercial Airplane Group and NASA Ames Research Center to achieve considerable increases in test Reynolds number using very large half-models in the NASA Ames 11x11 Unitary Wind Tunnel. This study developed the high Reynolds number test technology and demonstrated wing designs that were tailored for that high Reynolds number test environment.

II. Historical Background

The wind tunnel to flight scaling problem is not new. Large transports have always been tested at low subscale Reynolds numbers relative to flight, and a certain degree of technical risk has always been accepted. The scaling problem became more acute as transport wings became transonic, and experimental strategies to better simulate the flows were developed. Reference 1 presents an excellent overview of the recent state of the art of wind tunnel to flight scaling for transonic wings.

The historical background portrayed here is intended to follow the reasoning that was the basis for developing the methodology reported later in this paper. It is important to understand the background in order to understand the rationale for developing a new and expensive design and test technology.

Low Reynolds Number Environment

Most commercial jet transport aerodynamic wing testing has been accomplished in moderately sized atmospheric wind tunnels that can generate test Reynolds numbers that are an order of magnitude below the flight article. Figure 2 shows the flight Reynolds number spectrum of typical jet transports and shows data for the Boeing Transonic Wind Tunnel (BTWT). This wind tunnel is typical of that used in the industry. With a test section of 8 feet by 12 feet (2.44m by 3.66m) and atmospheric total pressure, a typical full model of a transport sized to 50% of the tunnel width can be tested at only 3 million Reynolds number based on wing mean aerodynamic chord. This compares to values up to 50 million for present large transports.

The two major *similarity parameters* involved in transonic wing design are Mach number and Reynolds number. Precisely matching Mach number has never been questioned with regard to wind tunnel testing. The physics of shock wave development and the determination of drag rise have always been central to this need. The desirability of achieving flight values of Reynolds number has always been recognized, but the urgency has never been as much as for Mach number. The physics of Reynolds number matching were not perceived to be as stringent as for Mach number, primarily because Reynolds number did not impose an operational limit on the aircraft as did Mach number. Designs that worked well at low Reynolds number generally worked better at high Reynolds number.

However, some aircraft developers encountered rude surprises at high Reynolds numbers that altered this thinking. Figure 3 is an example where a low Reynolds number wind tunnel evaluation of a configuration led to an under-

prediction of flight loads and led to a costly redesign and retrofit of a large number of airplanes. This work contributed to a better understanding of the physics relating low Reynolds number flows to high Reynolds number flows and eventually led to the concept of *aft transition fixing*. Figure 4 shows that the displacement effects of the boundary layer in flight can be reasonably well matched in a low Reynolds number wind tunnel by allowing the flow to remain laminar to the shock, as it might only at subscale conditions. The slower thickening of the laminar boundary layer prevents excessive boundary layer growth in the wind tunnel, better approximating the slow growth rate of the full-scale turbulent boundary layer. As long as the wing pressure distribution allows the needed laminar run, a reasonable simulation can be obtained by this technique. However, the boundary layer downstream of the shock may not be well matched by this technique. This can lead to a significant shock position movement relative to flight and can lead to problems similar to that shown in figure 3.

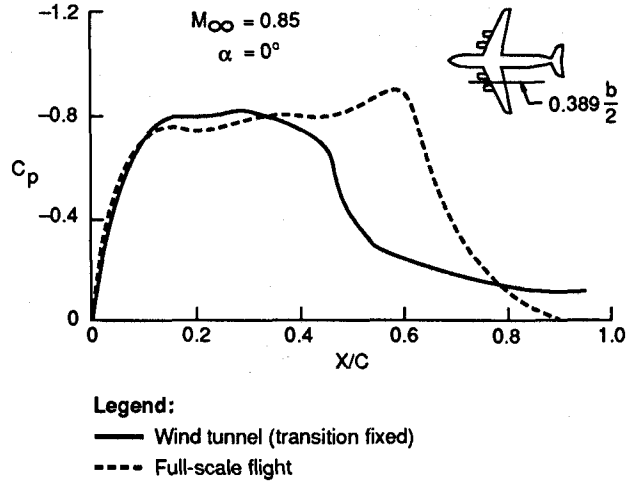

Figure 3. Example of Wind-Tunnel-to-Flight-Scaling Problem: C-141

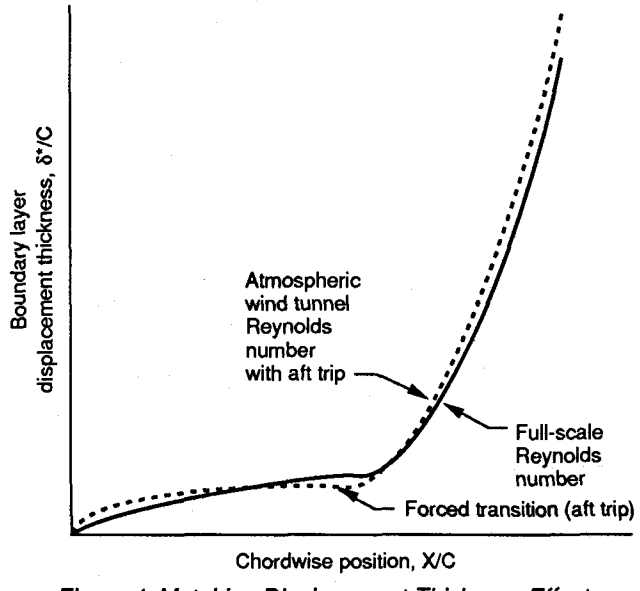

Figure 4. Matching Displacement Thickness Effects With Aft Tip

It should be mentioned that aft transition fixing is a central issue. Some experimenters have used natural transition to obtain even longer laminar runs at subscale conditions, but this leads to laminar boundary layer interaction with the shock, which can behave in a different manner than a turbulent interaction in flight. Specifically, laminar boundary layers can reattach after the shock (ref. 1).

Reference 1 discusses the possibility of matching parameters other than boundary layer displacement thickness between wind tunnel and flight Reynolds number. Boundary layer displacement thickness matching can be envisioned as an attempt to match the displacement effects of the boundary layer on the development of the outer flow. Work at ONERA (ref. 2) suggests that matching the physics of the laminar boundary layer interaction with the shock may be more important in wind tunnel to flight simulation.

Design Limitations of Low Reynolds Number

A central issue to this work is the fact that the design strategy for the wing can be influenced by the test Reynolds number. As discussed above, a fundamental precept of low Reynolds number simulation is the maintenance of a laminar boundary layer. However, this requirement puts a limitation on the design strategy for a wing. The fundamental parameters that affect the ability to maintain a laminar boundary layer include sweep, spanwise pressure gradient, and chordwise pressure gradient. It is the latter that has the most profound influence on the technology selection for a transport wing. Figure 5 schematically illustrates that the *architecture* of the chordwise pressure distribution can be limited by test Reynolds number. A neutral, proverse, or slightly adverse supersonic rooftop would be required for low Reynolds number aft trip evaluation to maintain the laminar boundary layer needed for flight simulation. The precise limit cannot be determined without the added knowledge of test Reynolds number, sweep, spanwise pressure gradient, and freestream turbulence.

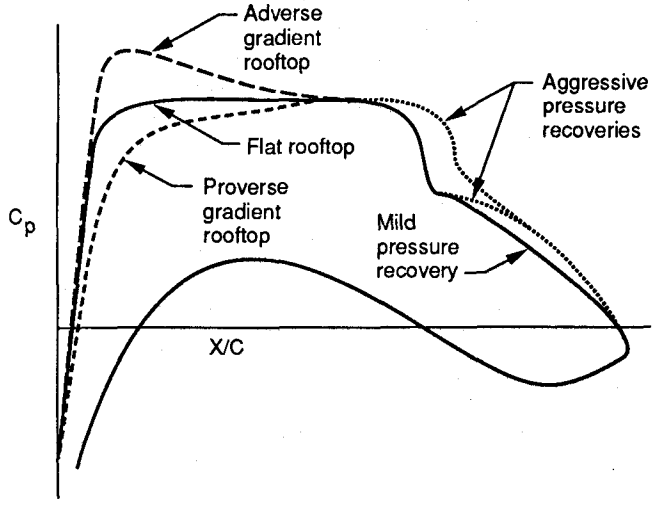

Figure 5. Pressure Distribution Architectures

Besides being able to simulate the *design condition* for a wing, the wind tunnel must be able to simulate off-design conditions as well. As shown in figure 6, a modern transonic airfoil exhibits a wide range of pressure distribution architectures depending on Mach number and lift coefficient. For many of these conditions, long runs of laminar flow would not be possible. Key off-design conditions that may not be simulated well include buffet, maximum lift, climb, and holding.

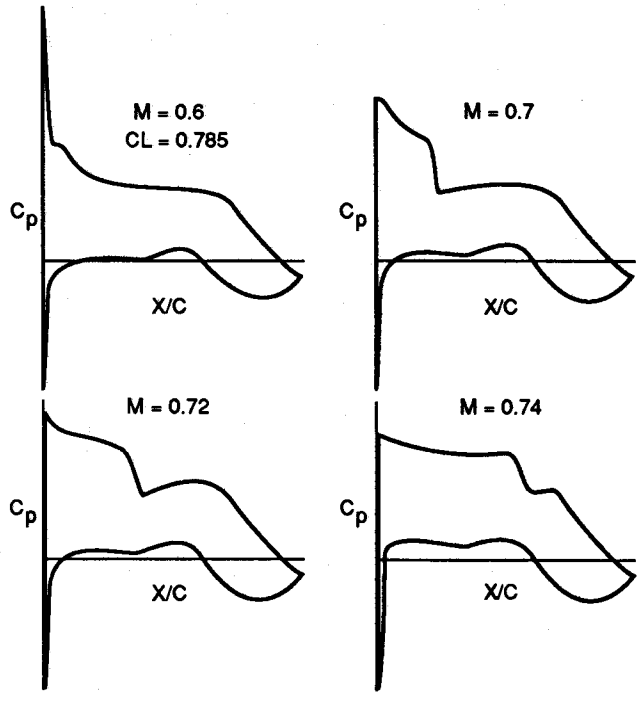

Figure 6. Changes in Pressure Distribution Architecture With Mach Number (Constant C_L)

Another key simulation problem at low Reynolds number is aft of the shock, as illustrated in figure 5. In this region the health of the turbulent boundary layer is a direct function of the test Reynolds number. It can only be controlled indirectly by *upstream boundary layer history*. Therefore, aggressive recoveries shown in figure 5 may not be achievable in a low Reynolds number test environment regardless of test strategy.

Higher Reynolds Number Environment

If a suitably high test Reynolds number environment can be found, many of the difficulties with simulation can be circumvented. The key is to test at a sufficiently high Reynolds number where a fully turbulent flow simulation gives a good representation of the flow physics on the full-scale article. A scientist may argue that only a full-scale representation would meet these criteria, and the cryogenic transonic wind tunnels may meet this need.

However, in this study an engineering approach to the problem assumes that major flow parameters can be reasonably well matched by a moderately high, but still subscale, test Reynolds number. Key to determining what test Reynolds number constitutes a good simulation is to first determine which flow parameters are important.

Good simulation requires that both the outer flow and the inner flow be matched well with full scale. The obvious flow parameters to match include the pressure distribution and shock location, the displacement thickness of the boundary layer, separation characteristics of the boundary layer, flow direction within the boundary layer, and perhaps the boundary layer shape factor. As the basis for this work, a CFD method was used to develop an understanding of the importance of each of these parameters. The method is based on the transonic full-potential wing/body method of Jameson (ref. 3) and the finite difference 3D boundary layer method of McLean (ref. 4).

A wing configuration designed to work well at low Reynolds number with an aft trip was also evaluated with fully turbulent flow over a broad spectrum of Reynolds numbers, including typical flight conditions for a commercial airplane of the 150-passenger class. As shown in figure 7, the computed boundary layer displacement thickness, trailing edge skin friction coefficient, and trailing edge flow angle vary with Reynolds number. The low Reynolds number aft trip simulation can match some but not all of the parameters. What is not shown, however, are flight conditions where the laminar flow cannot be maintained.

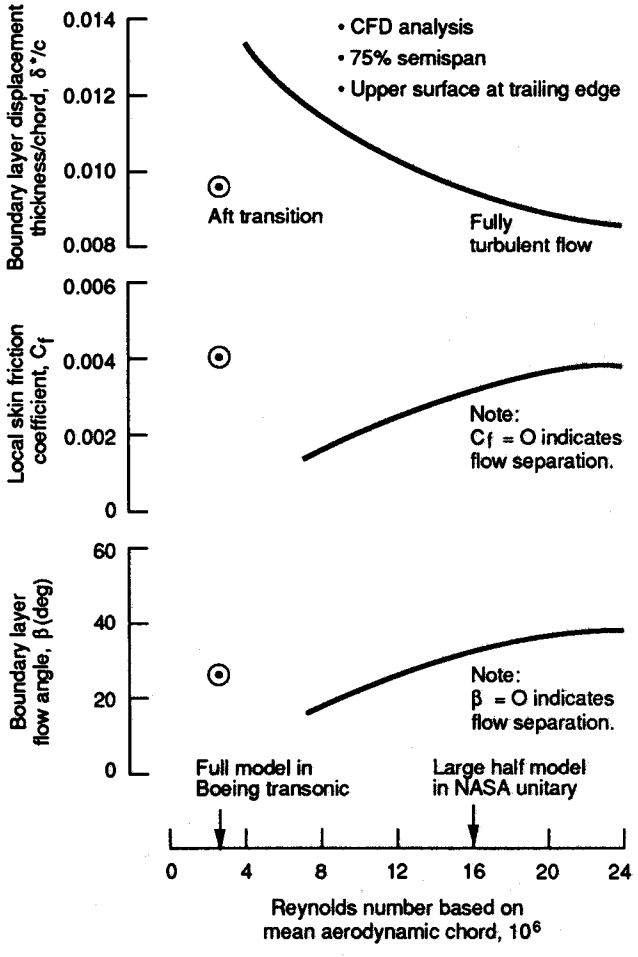

Figure 7. Effects of Reynolds Number on Boundary Layer Parameters

Figure 8 shows CFD predictions of the effects of Reynolds number on the outer flow. The CFD results predict that the outer flow pressure distribution is modeled fairly well with the low Reynolds number aft trip simulation. It is also well represented by fully turbulent flow as long as the Reynolds number is roughly 12 million or more. However, for lower Reynolds numbers the shock is shown to move forward, the rooftop elevates, and the subsonic recovery becomes weaker.

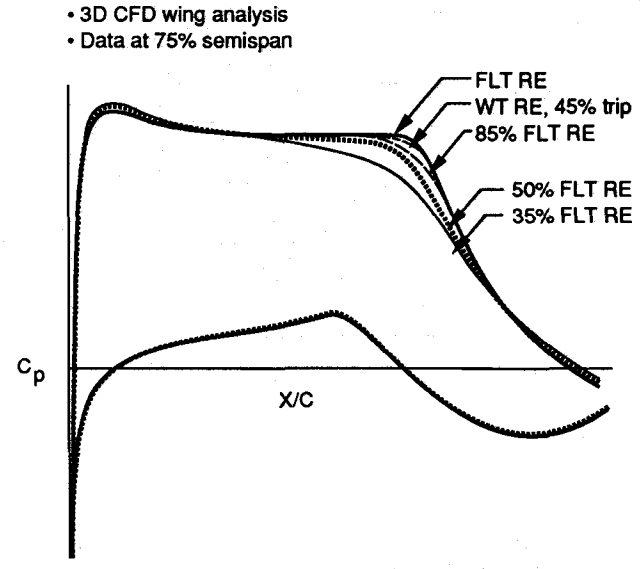

Figure 8. Effects of Reynolds Number on Pressure Distribution

The data shown for this case give reason to believe that a moderate Reynolds number, roughly 10 to 15 million, would provide a reasonable fully turbulent flight simulation of this particular wing. Other analyses, which are supported by the experimental work to be discussed later, support this finding for a broad class of transonic wings with relatively aggressive design pressure distribution architectures.

How Much Reynolds Number Is Enough?

The question of how much Reynolds number is enough cannot be answered simply. Factors such as the range of flight Reynolds number of the aircraft, the pressure distribution architecture, and the portion of the flight envelope of interest must be considered. Requirements for determining the cruise efficiency of the aircraft are different from that required to understand the edges of the flight envelope, stability and control characteristics, or structural design requirements.

Testing for the cruise efficiency of the aircraft is perhaps the easiest of the scenarios to understand, because attached boundary layers are to be expected. CFD can be used for this class of flows, and the type of analysis described above can provide considerable insight into the Reynolds number requirements for a given wing technology.

In the future, a complete set of wind tunnel data, including pressure distribution and boundary layer data, may be obtained using the new cryogenic wind tunnels. These data, along with similar information from flight tests, may help quantify the needed test Reynolds number to obtain good flight simulation in routine developmental wind tunnel testing.

III. High Reynolds Number Test Capability

The previous discussion has summarized the reasoning used to embark on developing a moderately high Reynolds number wind tunnel test capability that can be used for the high volume of testing typically used to develop a commercial transport. Historically these airplane development programs have invested thousands of hours of wind tunnel time over the course of several years, requiring the use of very productive wind tunnels. Typical commercial transport development programs examine 20 or more wing designs.

The following discussion summarizes the major issues examined in developing the test capability.

Concept Selection

With a test Reynolds number range of 10 to 15 million based on wing mean aerodynamic chord as a goal, the major issues involved in selecting a test concept are facility productivity and availability, test medium, full or half model, wall configuration, cost, and location.

An inventory of the world's transonic wind tunnels available for commercial testing reduced the list to only a few possible choices: NASA Ames 11x11 Unitary, NASA National Transonic Facility, AEDC 16T (USAF), NAE (Canada) 5x5, RAE (United Kingdom) 8x8, and Calspan 8x8.

Only the NASA NTF would allow sufficiently high test Reynolds number with a full model, and the developmental state of this wind tunnel at the time eliminated it from contention. Thus, the decision to test with half-models became mandatory if the Reynolds number range were to be reached. The other factors described above led to the technical decision to concentrate this work at the NASA Ames 11x11 Unitary Wind Tunnel in Mountain View, California, U.S.A. The tunnel is shown in figure 9.

Key Technical Issues

A number of key technical issues were addressed to develop the capability to routinely achieve test Reynolds numbers of approximately 15 million at Mach numbers up to approximately 0.9. A brief summary of each issue is discussed below.

Model Size Selection: The half-model decision described above was based on attainment of test Reynolds number requirements. Reynolds number is the only motivation for selecting a half-model. Other facets of half-model testing are generally negative, and the added burden of a half-model cannot be easily justified otherwise. Cost and model fidelity are other reasons why half-models are often chosen, but these were not factors in this work. The actual size of the half-model was selected based on anticipated wall effects and blockage effects. To achieve the desired 15 million Reynolds number, the half-model would span nearly 75% of the Ames wind tunnel and would be of roughly 2.5% solid blockage.

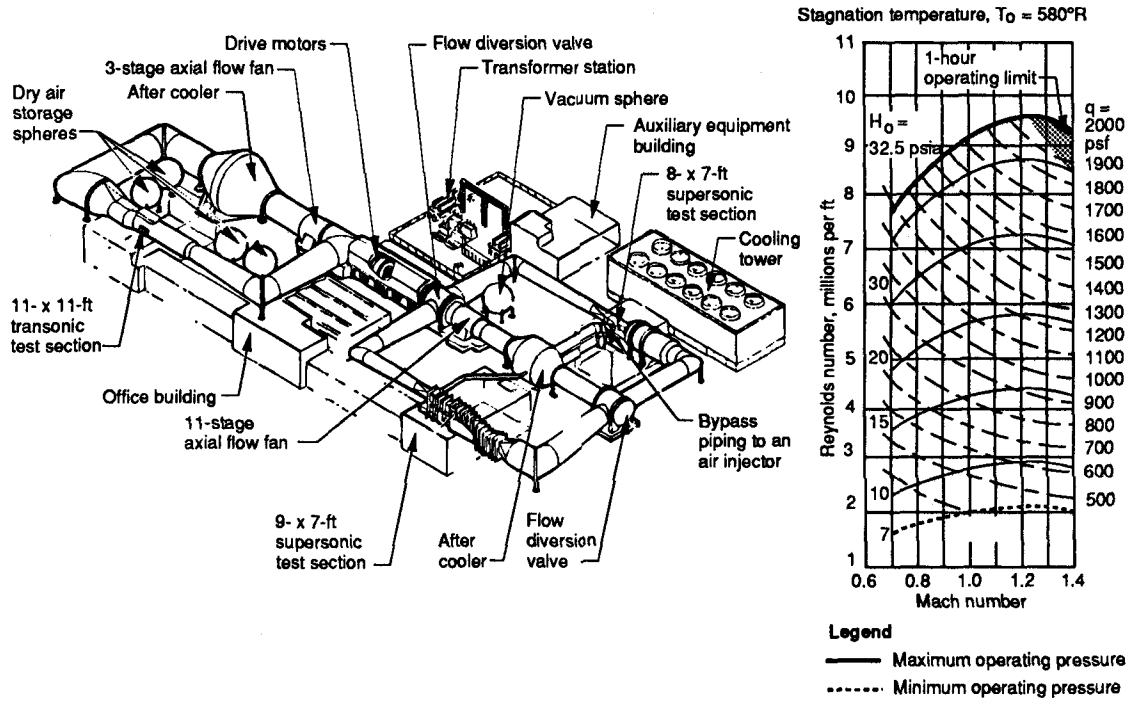

Figure 9. NASA Ames Unitary Wind Tunnel

Wall Effects: Considerable analyses were conducted to satisfy technical concerns relative to wall effects. A CFD model based on the work of reference 5 was assembled using the linearized subsonic potential flow method of reference 6. This CFD representation modeled the slotted walls of the Ames wind tunnel with homogeneously porous walls as shown in figure 10. At first using an assumed porosity factor derived from previous studies of reference 5, and later verified by measuring wall pressures as depicted in figure 10, the wall-induced disturbances on the wing were computed. A fundamental requirement was that the wall effects be correctable. That is, simple angle of attack and Mach number corrections can be used to account for the constraining effects of the walls. Large spanwise or chordwise gradients, which are not correctable, were not allowed.

Figures 11 and 12 summarize the findings for the model size ultimately selected. Figure 11 shows that streamwise angle of attack gradients of no more than 0.01 degrees were computed. Spanwise gradients of a similar order of magnitude were also obtained. Both of these effects were deemed insignificant. Figure 12 shows that streamwise Mach gradients of less than 0.002 could be caused by the wind tunnel walls, while the spanwise gradient could be as large as 0.005. These effects were later shown to be insignificant as a result of testing different sized models at the same Reynolds number at a typical cruise operating condition. (This may not be true at more extreme conditions, such as near buffet onset, where the wall effects could become transonic and nonlinear.)

In assessing these wall effects, a key consideration was that the wall-induced aerodynamics should not change the character of the flow on the wing. Small gradients, as noted above, might be tolerable as long as the basic pressure distribution architecture and flow physics are preserved. Figure 13 summarizes data acquired on three test articles

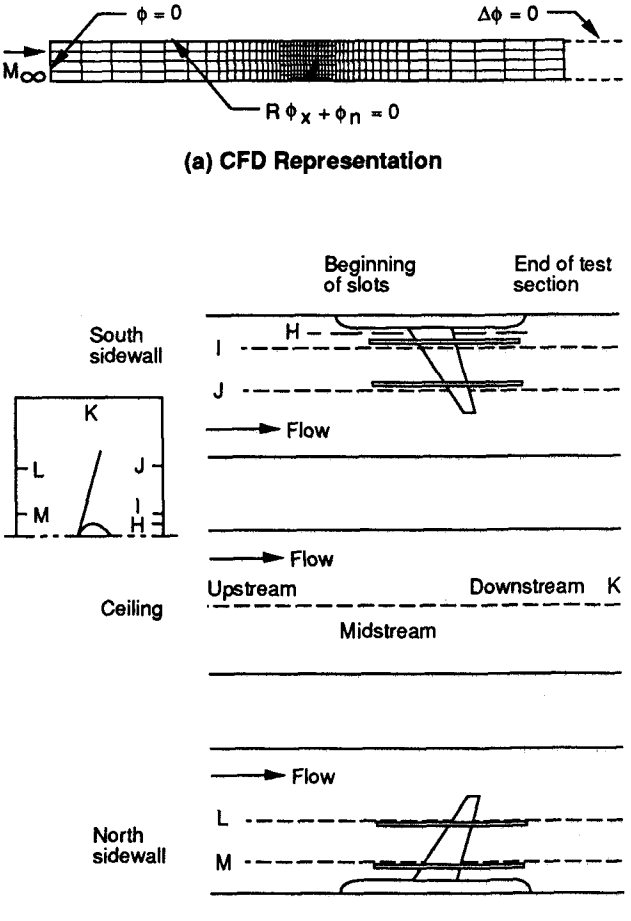

Figure 10. Wall Interference Assessment

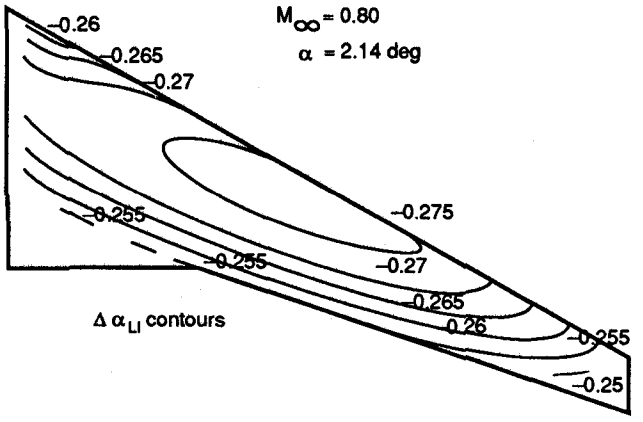

Figure 11. Wall-Induced Flow Curvatures

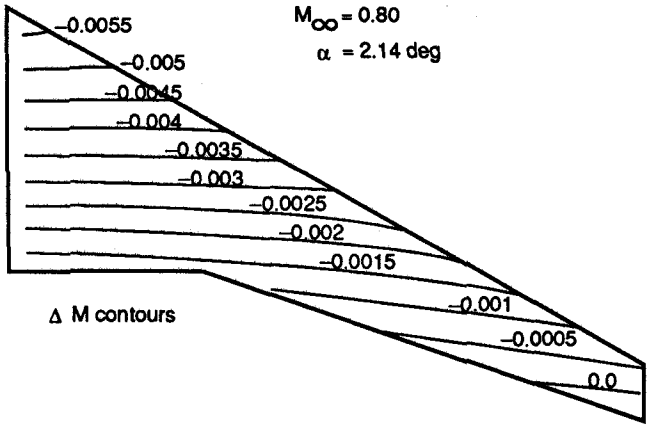

Figure 12. Wall-Induced Mach Contours

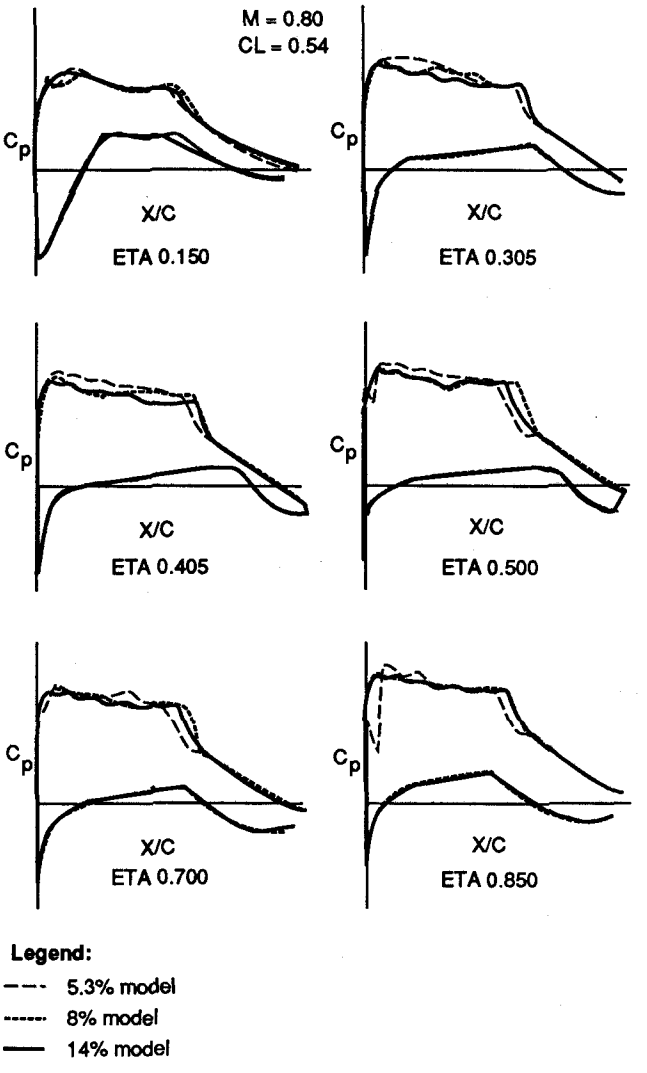

Figure 13. Experimental Assessment of Wall Effects

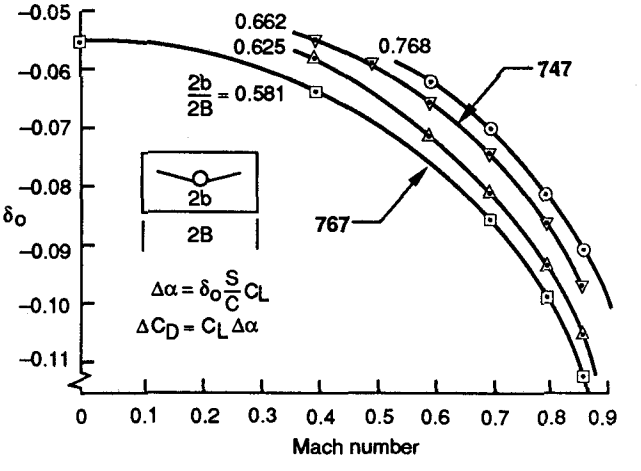

Figure 14. Lift Interference Correction

representing the same geometry at different model scale. Each was tested at the same chord Reynolds number in the NASA Ames 11x11 as a half model. It can be seen that the character of the pressure distribution is well replicated at each model scale, with only a small deviation near the wingtip for the smallest model, probably the effects of model aeroelastics.

It has been stated that the wall effects should be represented by relatively simple corrections to angle of attack and Mach number. The CFD work, supported by the measured wall pressure distributions, resulted in wall effects corrections as shown in figures 14 and 15. Figure 14 shows that the *lift interference* term varies with both model span and test Mach number, typical of that shown in reference 5. Figure 15 shows that *solid blockage* varies primarily with test Mach number only. Blockage also results in a streamwise pressure gradient, which can be inferred from figure 12. This *solid blockage buoyancy* results in a large drag term, which must be included in wall corrections as well.

Half-Model Effects: Testing a half-model introduces a new set of problems related to interaction with the floor boundary layer and to mechanical interference with the floor. The effective reflection plane for a half-model installation is somewhat above the wind tunnel floor because of the displacement effects of the floor boundary layer. However, growth of the floor boundary layer is influenced by the model. From an outer flow standpoint, it would be desirable to seal the half-model to the wind tunnel floor, but in order to use a force balance it is necessary to provide

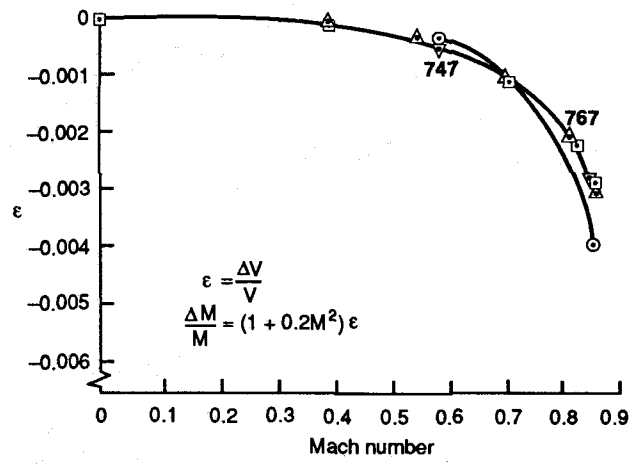

Figure 15. Blockage Correction

mechanical clearance from the floor for all anticipated test conditions. These requirements, therefore, are contradictory.

The displacement thickness of the floor boundary layer in the Ames wind tunnel at its maximum operating total pressure of 65 inches (2.2 bars) of Mercury was measured to be roughly 0.6 inches (15.2 mm). It is not clear at what model centerline height the best reflection effects would be obtained. However, at one displacement thickness above the floor the fuselage centerline would see roughly 65% of freestream flow velocity. At two displacement thicknesses roughly 90% freestream flow velocity would be present. Mechanical clearance requirements were somewhat less than the 0.6-inch (15.2-mm) value.

For this work, the model was actually placed such that its centerline was 1 inch (25.4 mm) above the wind tunnel floor in nearly freestream velocity flow. The gap beneath the model was then filled with a *fuselage profile plate*, which closed the gap to about 0.5 inches (12.7 mm), and a *centerline dam*, which further closed the gap to 0.1 inches (2.54 mm) over most of the model length to inhibit flow from the pressure side to the suction side of the model.

Figure 16 compares pressure data measured on a small version of the half-model and on the same hardware tested as a full model at the same Reynolds number. Excellent agreement is shown, confirming at least the validity of the reflection plane assumption.

A deficiency of the half-model simulation, however, is in the measurement of force data. The underside of the model and the mounting pedestal for attaching the model to the underfloor balance are both *metric* surfaces in this installation. The presence of these surfaces contaminates the data, particularly the drag data. However, as shown in figures 17 and 18, respectively, the shape of the drag polars and the shape of the drag rise are well represented in the half-model simulation, where comparison is shown to full-model data.

A more sophisticated half-model mounting system would involve a nonmetric fuselage profile plate and windshield for the mounting pedestal. The mechanical aspects of this type of mounting system discourage its use. These half-model issues are discussed at length in reference 7.

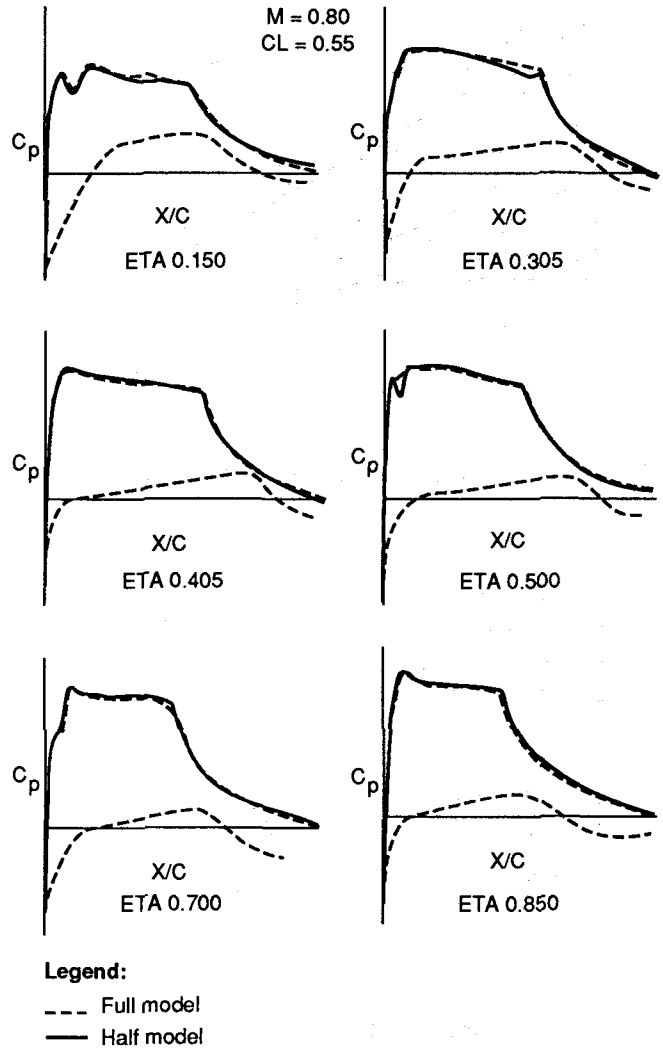

Figure 16. Experimental Assessment of Half-Model Effects

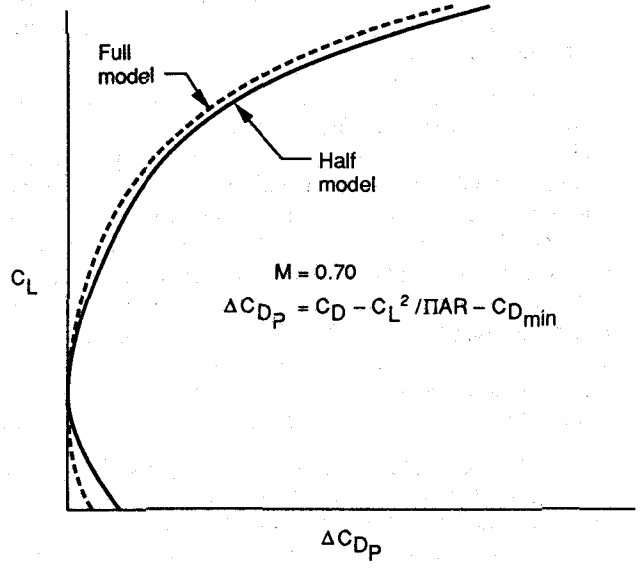

Figure 17. Drag Polar Shape From Full and Half Models

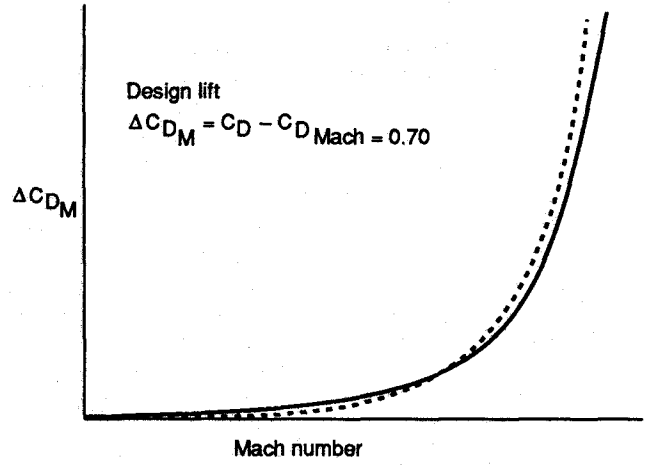

Figure 18. Drag Rise Shape From Full and Half Models

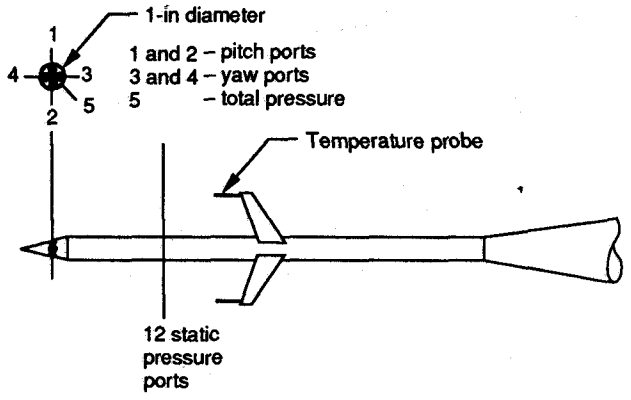

Flow Calibration Probe

Wind Tunnel Flow Environment: The flow environment of the test facility must also be known for precision wind tunnel testing. The NASA Ames 11x11 Unitary Wind Tunnel has been used primarily for testing sting-mounted full models. Little was known about the wind tunnel for half-model testing, including Mach number calibration with the floor slots sealed and crossflow angularity.

As part of this testing technology development program, tunnel flow characteristics were measured. Using a multipurpose flow probe shown in figure 19, it was determined that a change in tunnel Mach number calibration from the fully ventilated configuration was required, also shown in figure 19.

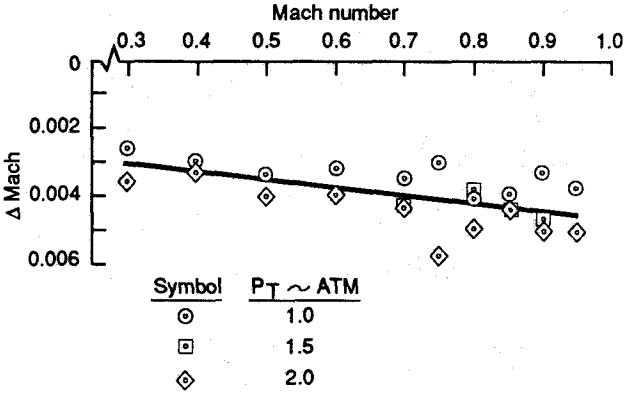

Δ Mach = Half-model configuration – full-model configuration

Figure 19. Mach Calibration for Half-Model Testing

A disturbing flow characteristic discovered in this calibration phase was a crossflow distribution as shown in figure 20. For half-model testing this crossflow can be regarded as an effective twist distribution imposed on the wing of nearly 0.7 degrees! Concern about this crossflow irregularity were high enough that a symmetrical wing and body pressure model was constructed and tested as a tunnel calibration exercise. Figure 21 summarizes the results from the symmetrical model testing. It shows that the crossflow is manifested differently for lift and for drag. Using a mean crossflow that gives zero lift at zero angle of attack results in an asymmetric polar. Using a mean crossflow that gives a symmetrical drag polar results in approximately 0.1-degrees zero lift angle of attack. This anomaly between lift and drag is a result of the effects of the flow distortion and its interaction with the wing spanloading. It can be regarded as a *freestream induced drag*. It is the same effect as depicted in reference 8, figure 13, for changes in drag resulting from a spanwise variation of flow angle.

The flow distortion problem depicted in figure 20 is presumed most likely to be caused by a fixture used for tunnel calibration tests, which is permanently mounted to the turning vanes in the corner of the Ames wind tunnel immediately upstream of the test section. If this presumption is correct, the long-term plan is to remove this fixture. In the meantime, the symmetrical model data summarized in figure 21 are being used as a means of correcting wind tunnel data obtained in the present test environment.

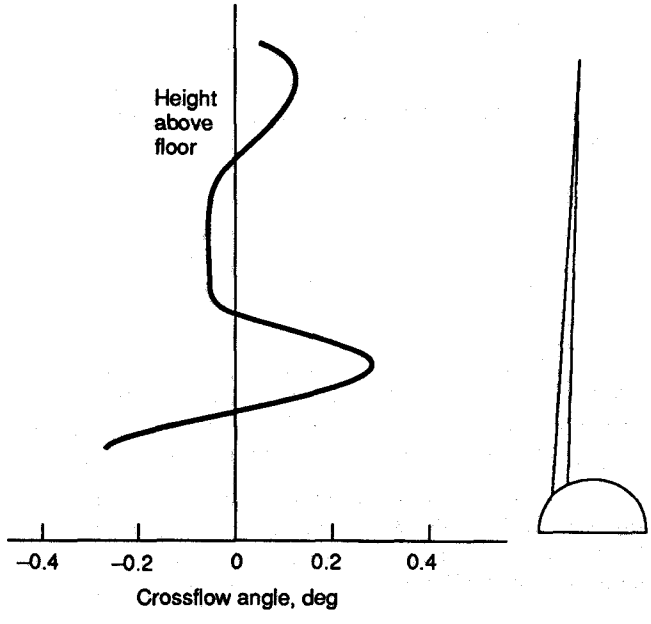

Figure 20. Measured Wind Tunnel Crossflow Distribution

Measurement Issues: Some major wind tunnel data measurement issues were investigated as part of this testing

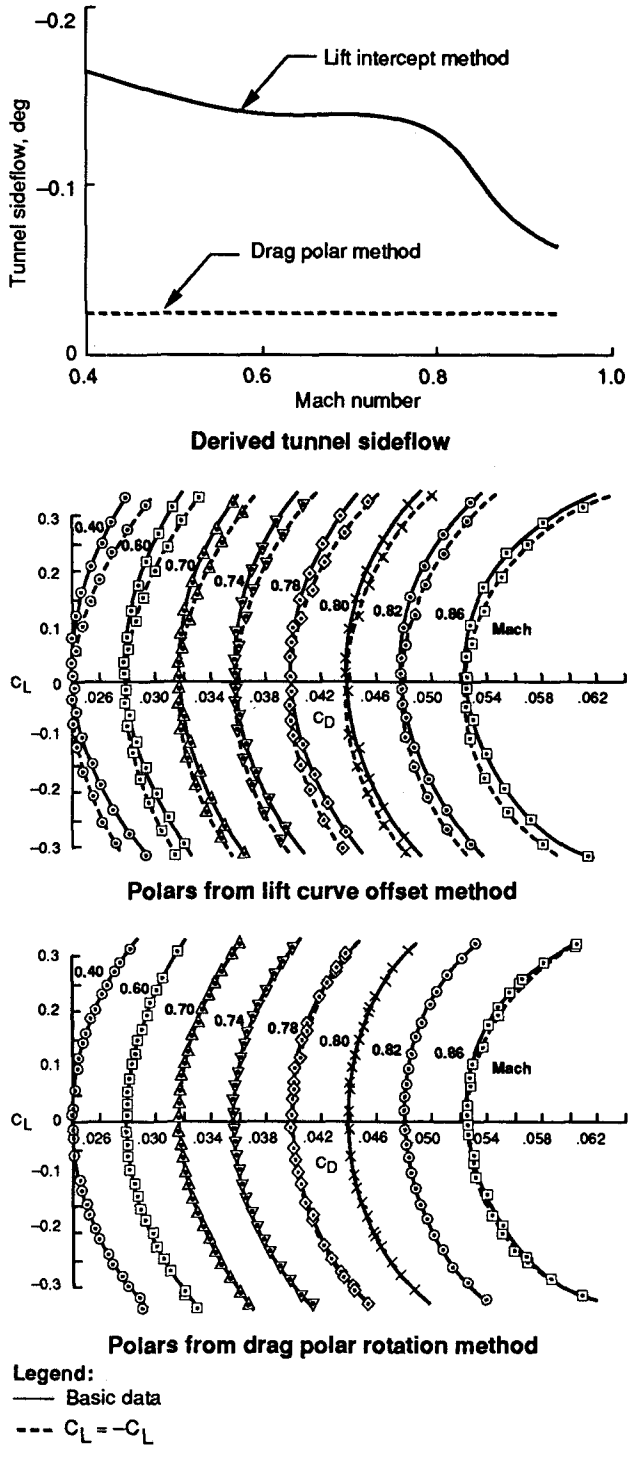

Figure 21. Symmetrical Model Crossflow Determination

technology development program. Specific issues that are peculiar to the large half model installed in the NASA Ames 11x11 Unitary Wind Tunnel include very large force balances, angle of attack measurement, and flow visualization.

Because of the large model scale and the pressurization capability of the wind tunnel, uncharacteristically large forces and moments are generated by these wind tunnel models. The model is mounted on a turntable under the tunnel floor within the pressure vessel, which results in very large forces and moments that must also be absorbed by the test section structure.

Two five-component strain gage balances are available for this testing. Table 1 summarizes the force and moment capacities of these balances. Design features incorporated into both balances include temperature compensation and temperature calibration. Temperature compensation means that the balance has been instrumented to minimize the effects of temperature and temperature gradient changes due to thermal expansion of the flexures. Temperature calibration means that any residual temperature or temperature gradient induced changes in the balance sensitivities are included in the calibration process. During testing the balance *zero return* histories were recorded, and these large balance exhibited less than 0.1% deviation between beginning and ending wind-off zeroes. For axial force, the most sensitive component, this amounts to approximately one-half drag count (0.00005 drag coefficient).

Balance capacities		
Component	Boeing 5240	Ames hi-q
Normal force (lb)	27,000	25,000
Axial force (lb)	1,400	2,000
Pitch (in-lb)	192,000	150,000
Roll (in-lb)	924,000	750,000
Yaw (in-lb)	51,000	80,000

Table 1. Half-Model Balance Capacities

Angle of attack measurement is always a crucial issue. In this case, it is particularly important because the force resolution into lift and drag depend intimately on balance to freestream angle. An uncertainty of 0.01 degrees results in a drag uncertainty of one drag count at typical cruise conditions.

An angle of attack system was developed for this installation which achieved the required accuracy. Central to the installation was that the angle measured was that of the *metric* side of the balance. By using the metric side any balance deflections in pitch resulting from applied loads would be measured directly by the instrumentation. Precision rotary encoders were mounted to rigid tunnel structure under the test section, and these encoders were attached to the balance metric face using torque tubes extending through the center of rotation of the balance. A dual system was installed using concentric torque tubes to provide a backup and to identify problems quickly.

Another key aspect of the angle of attack measurement problem was involved with obtaining a reliable means of determining zero angle. Because the model is mounted vertically from the wind tunnel floor, gravity cannot be used to establish a reference zero. Rather, an optical system was developed using a transit, a model mounted alignment fixture, and tunnel reference points. Extreme care must be taken to ensure that the reference zero angle has similar precision to the encoder capability.

Flow visualization is a major source of information to a wing design aerodynamicist. In a pressurized wind tunnel environment, however, access to the model is very limited. Accomplishing meaningful flow visualization experiments, therefore, requires significant preplanning. For these experiments ultraviolet oil flow visualization was the primary approach to visualizing wing surface flows. A suspension of UV dye in motor oil was stored in a reservoir, and this was dispensed from a network of embedded tubes near the wing leading edge. Using five plenums, oil was dispensed though these tubes from small holes drilled at 0.5-inch (12.7-mm) intervals. Figure 22 is a typical example of the resulting flow visualization. Cameras were mounted inside the pressure vessel behind the test section sidewalls. These cameras and UV strobe lights were controlled remotely and coordinated with the oil dispensing operation.

IV. Wing Design

As discussed earlier, the underlying reason for developing the wind tunnel testing methodology to routinely obtain very high Reynolds numbers is to allow higher technology wings to be designed. Along with the benefits of increased test Reynolds number, computational fluid dynamics (CFD) provides the capability to design, to a much higher degree of refinement, three-dimensional wings that can take advantage of this improved test environment.

Transonic and viscous wing CFD methodology has reached a very high level of maturity in recent years. These algorithms along with very high capacity supercomputers and engineering workstations have revolutionized the aerodynamic wing design process. However, with the ability to acquire high Reynolds number wind tunnel data, it became apparent rather quickly that the previous *calibration* of the CFD tools to wings designed and validated at low Reynolds numbers was not sufficient for the more advanced wings intended for high Reynolds number evaluation. CFD codes and design philosophies had to be modified as results of this testing were obtained. In fact, the process is continuing. An overview of the wing analysis and design process and some findings are presented in the following sections.

CFD Methods

The state of the art of transonic/viscous wing/body analysis and design is probably more highly developed than any other area of computational aerodynamics. The reasons for this are simply that the problem is both crucial to airplane design and is generally solvable. The flows are generally characterized by weak shock waves and fully attached boundary layers, both of which are within present CFD capabilities. This is not to say that the problem is trivial and that all aspects of the problem are solved. In fact, the work presented herein has identified a number of shortcomings of the present methodology and has initiated additional work to continue to improve the state of the art.

The work of Jameson (ref. 3) is recognized throughout the world community of CFD developers and appliers as the primary building block for transonic wing design. The method is a finite difference solver of the *full potential equations* for a large class of wing and body configurations with transonic flow. In the Boeing code, viscous effects are included in the wing portion of the solution by accounting for the displacement effects of the boundary layer using the 3D finite difference code by McLean (ref. 4). Figure 23 describes the iterative technique used to couple the inner and outer flow solutions. Typically, a dozen cycles between the full potential and boundary solutions are required to achieve convergence. On a Cray X-MP supercomputer an analysis solution of this type requires approximately 3000 CPU seconds.

Similarly, the *inverse* or design problem is solved using a Jameson code with a mixed boundary condition, as depicted in figure 24. The inverse problem is solved inviscidly, but the designed wing shape includes an embedded boundary layer. The actual wing geometry is

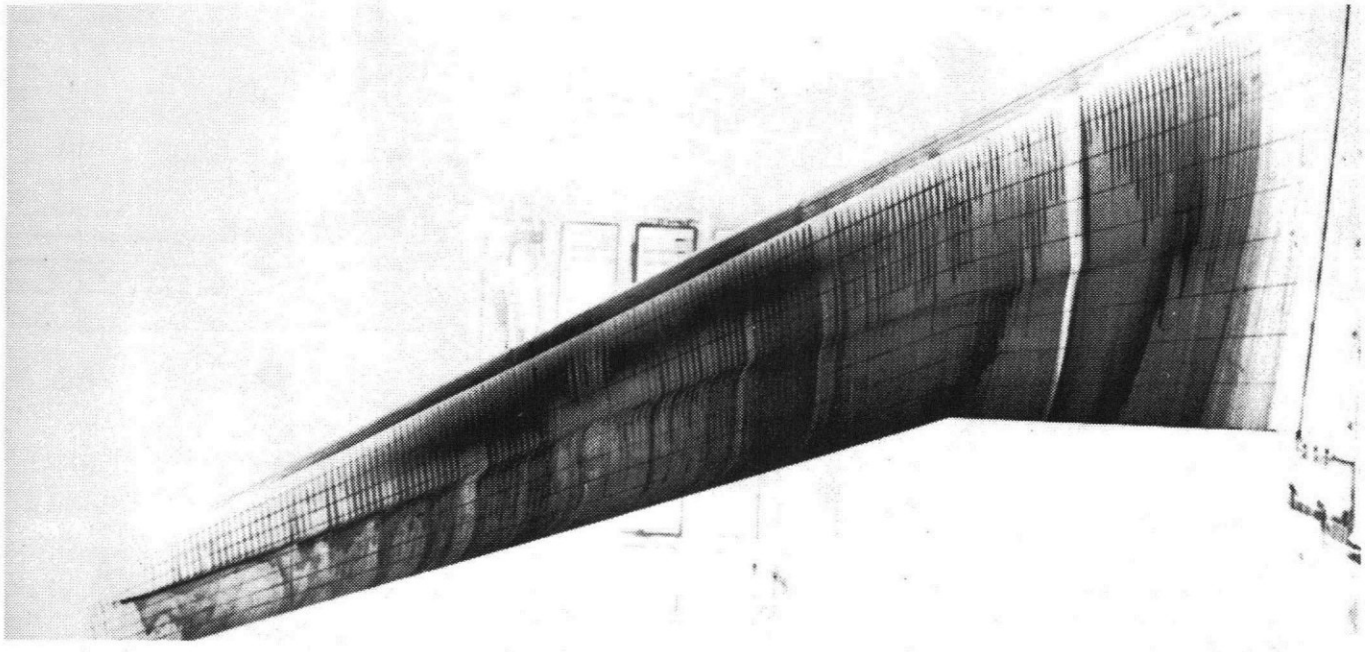

Figure 22. Flow Visualization Using Ultraviolet Oil Dispensed From Onboard System

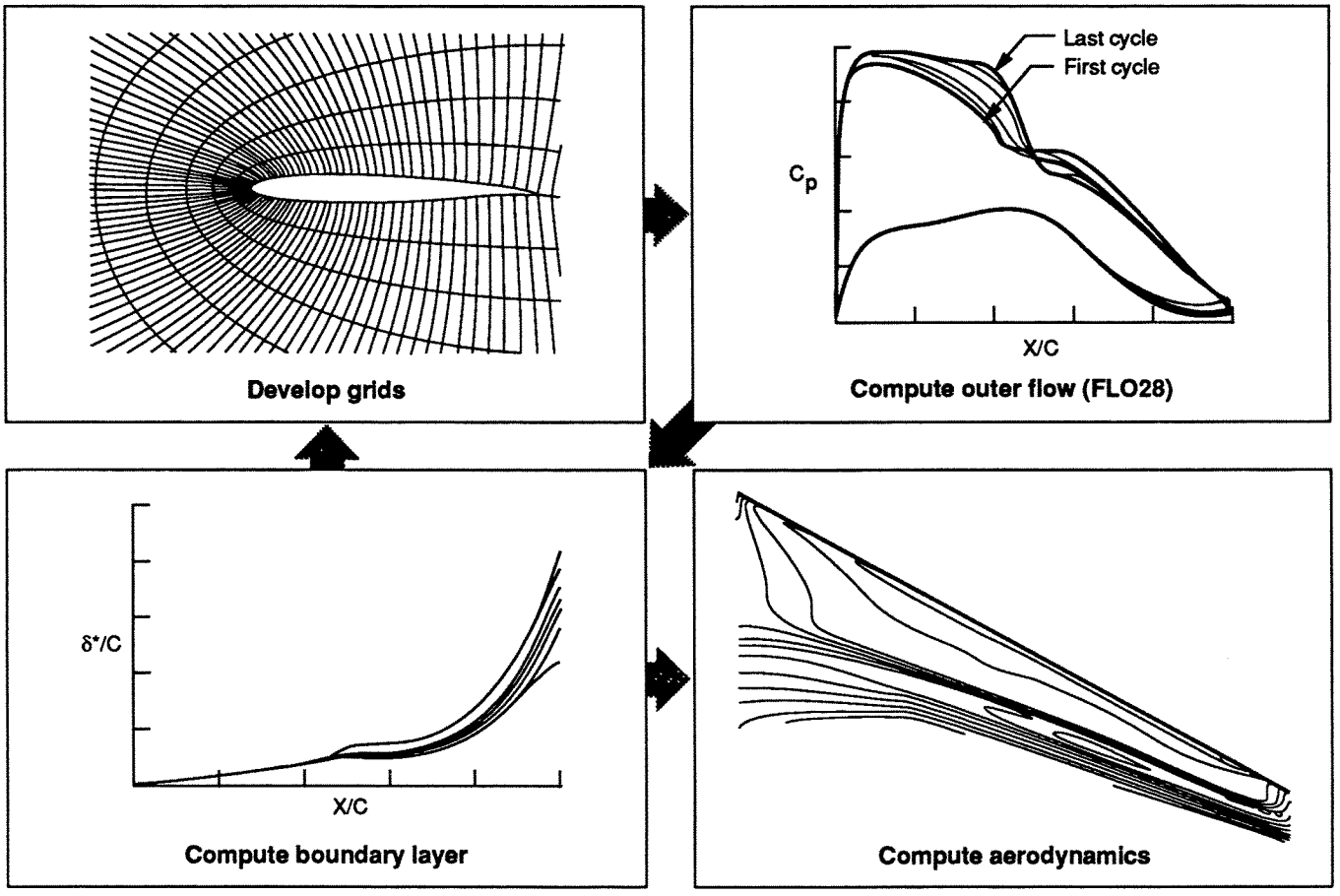

Figure 23. Transonic/Viscous Wing/Body Analysis Process

obtained by removing a computed displacement thickness after the inverse solution is complete. While figure 24 gives the impression that the inverse problem is quite simple, in practice it is a very complex problem requiring many cycles of smoothing, blending, and respecifying pressure distribution goals. Inverse wing design is a good technique for establishing the overall character of the three-dimensional wing pressure distribution. However, the final wing design, which includes geometric as well as aerodynamic considerations, requires considerable manual iteration in the direct analysis code.

Design Freedoms At High Reynolds Number

Removing the restriction of having to design a wing pressure distribution to allow a laminar run to exist at low Reynolds numbers in order to provide a good simulation of flight conditions opens the design space to the aerodynamicist. In addition, the higher test Reynolds number environment may also allow more adverse pressure gradients to be acceptable for a fully turbulent boundary layer. As shown previously in figure 5, the pressure distribution architectures allowed by the higher test Reynolds number may be significantly more aggressive than that required for testing in conventional facilities.

Depending on the design application, the added capability shown schematically in figure 5 can be used to design a faster wing for the same structure; a thicker or less swept wing for the same Mach capability; a wing with higher lifting capability; or a combination of any of these. In any event, the capability allowed by the higher test Reynolds number should result in a more competitive product with more mission capability to the airplane operator. The keys to achieving these technology advances are aggressive pressure distribution architectures, advanced CFD techniques including 3D inverse capabilities, and a high Reynolds number test environment.

Inverse Design Techniques

While the concept of designing wings using inverse codes has been available for some time, when applied to more aggressive designs allowed by the high Reynolds number environment some new problems can arise. To achieve significant isentropic recompression in the supersonic rooftop as shown schematically in figure 5, the design codes tend to flatten the airfoil upper surface over a significant portion of the chord. These very long regions of low curvature are very sensitive to small changes in the flow, and hence they tend to exhibit rapid changes in the pressure distribution architecture for *off-design* conditions. The problem is exacerbated as the design shock location is moved aft, and the geometry needed to close the airfoil results in a curvature concentration that can spawn a second shock. An example of this is shown in figure 25, which is experimental data from an outboard section of a wing tested at high Reynolds numbers in the Ames Unitary Wind Tunnel. While the design condition provides many of the desired features of an advanced pressure distribution architecture,

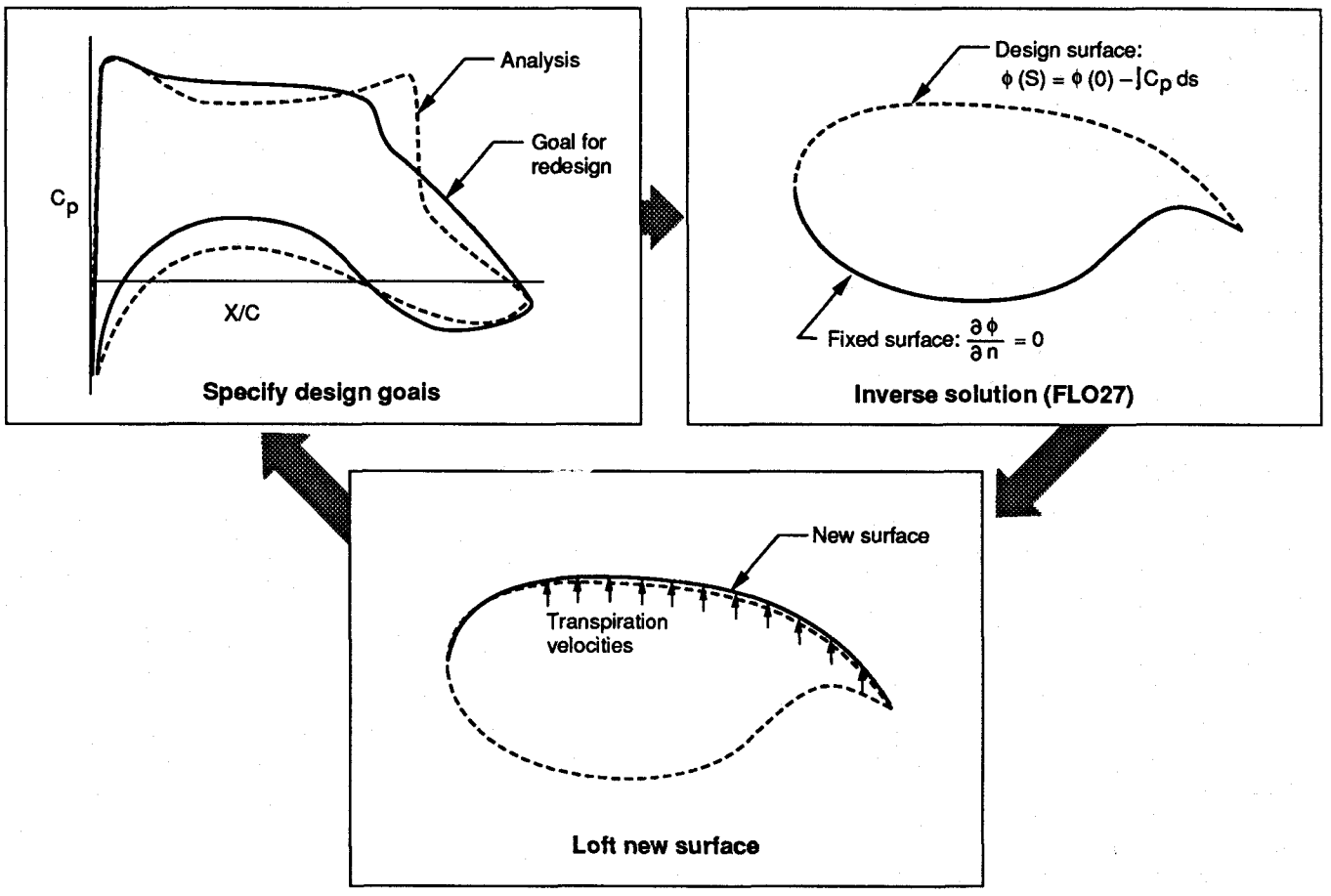

Figure 24. Transonic Wing Design Process

when either Mach or angle of attack are perturbed the character of the pressure distribution becomes very undesirable.

This problem was particularly disturbing in the early phases of this research work. Another lesson, which was learned by unfortunate experience, was that the CFD methods required considerably more grid density in order to resolve some of these off-design features that proved to be unacceptable. For the more benign designs that had been routinely produced for a number of years, the *standard* grid densities used produced excellent code/test correlations over wide ranges of Mach and angle of attack. However, more aggressive wings as depicted in figure 25 brought out new CFD deficiencies.

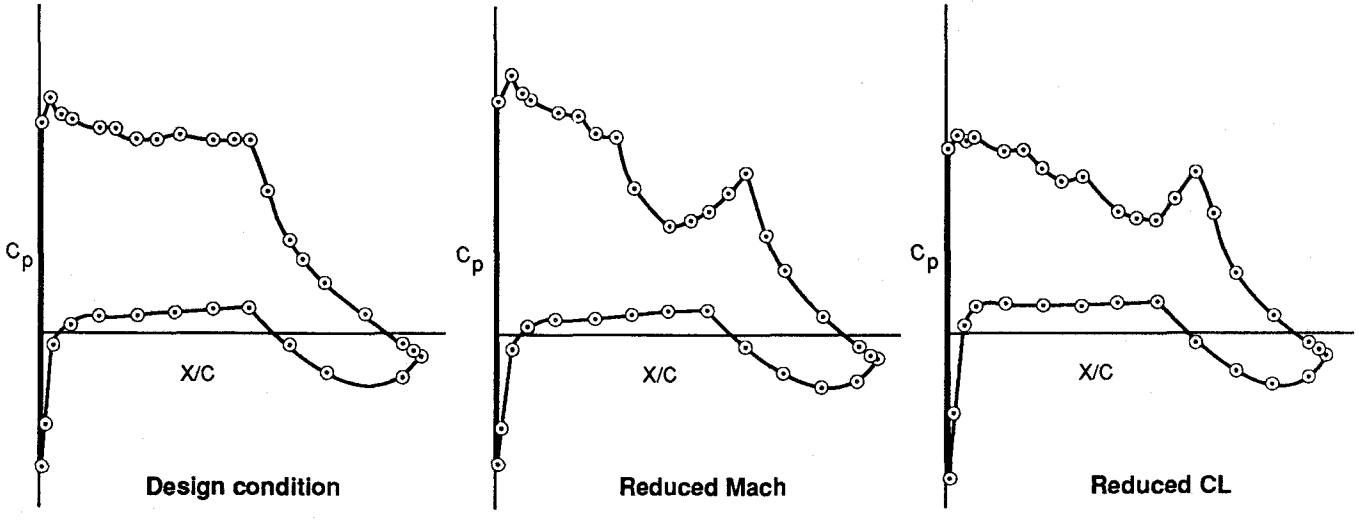

Figure 25. Outboard Wing Pressure Distribution Development

Once the code modeling had been upgraded to identify problems depicted in figure 25, a procedure was developed and later verified by testing at NASA Ames to achieve an aggressive pressure distribution architecture with reduced off-design problems. By choosing several flight conditions for inverse design, including the cruise condition and several other key conditions, it is possible to develop a compromised wing that exhibits most of the performance gains of the single-point design without the undesirable features shown. Figure 26 shows a similar set of pressure distributions from testing an improved wing. The previous tendency of the flow to re-expand after the shock has been tempered by the multiple design point strategy. The wind tunnel measurements show that this improved wing has superior drag characteristics, both on- and off-design.

CFD Improvements

In addition to the multiple design point philosophy and increased CFD grid density findings discussed above, other CFD advances have come from this study. In particular, the viscous model used in the CFD codes consistently predicted boundary layer separation much earlier than encountered in testing at high Reynolds number. This early breakdown of the boundary layer during the design process limited the aggressiveness of the designs.

By obtaining and analyzing large amounts of flow visualization and pressure data and examining in detail code/test correlations, improvement in the CFD viscous model have been made. Changes to both the eddy viscosity model in the method of reference 4 and to the coupling of the inviscid and viscid models near the wing trailing edge resulted in an improved CFD method. The method gives improved pressure distribution correlation and also provides a more realistic assessment of the onset of trailing edge separation.

Technology Advances

With improved test techniques and CFD codes and applications, further wing technology advances will be possible. Even more aggressive pressure distribution architectures can be implemented because of the improved CFD viscous model. Alternate 3D design strategies can be explored with the improved CFD models because a high level of confidence can be placed in achieving the design goals. Also, innovative wing technologies, such as laminar flow, variable geometry, and special trailing edge treatments can be assessed with confidence in conditions nearing flight.

V. Conclusions

Wing design technology advancements have been achieved by designing and testing at very high Reynolds numbers. CFD has played a major role in this work by allowing more aggressive wing designs to be developed and also by allowing much larger wind tunnel models to be tested with confidence. Design strategies have been developed that provide wings that work well over a wide operating envelope. These wing designs have been compromised to provide practical geometries suitable for manufacture. The test technique provides validation of the designs in a flow environment approaching flight conditions, thereby reducing some risk inherent in subscale validation. Some risk is introduced, however, by the present need to test half-models. As more capable wind tunnels are built, this risk can be mitigated.

The wing technology can be used to develop a more efficient airframe, depending on mission requirements. For a given structural arrangement a faster airplane can be developed. Or for a given Mach number capability a lighter more efficient structure can be developed.

Through the use of integrated CFD and high Reynolds number design and test, another increment of wing aerodynamic technology has been demonstrated. Investment in this technology has provided additional design freedoms in configuring an airplane and allows for improved performance and mission capabilities.

VI. Acknowledgments

Many individuals contributed to this effort. At NASA Ames Research Center, personnel from the Aerodynamic Facilities Branch and Applied Aerodynamics Branch were

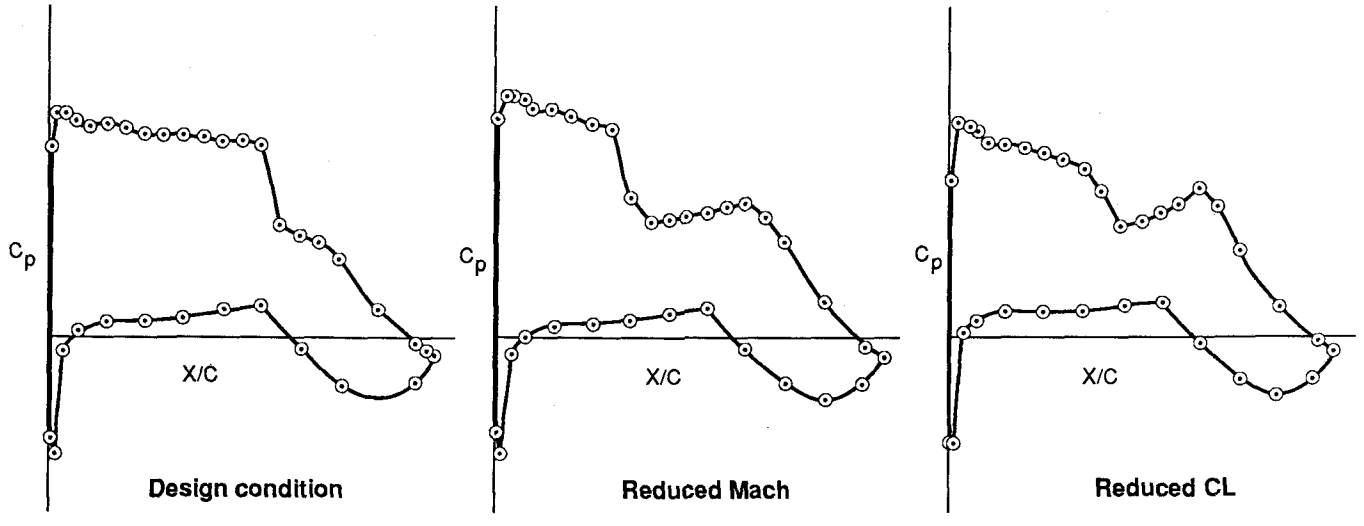

Figure 26. Improved Outboard Wing Pressure Distribution Development

involved in all aspects of developing test techniques, wall corrections, and in acquiring test data. At the Boeing Commercial Airplane Group, personnel from the New Airplane Division Aerodynamics Engineering Unit were responsible for all aspects of this work. Personnel from the Boeing Aerodynamics Laboratory and the Boeing Aerodynamics Engineering Research Unit also contributed to this effort.

VII. References

1. A. B. Haines, 27th Lanchester Memorial Lecture, "Scale Effect in Transonic Flow." Aeronautical Journal, August-September 1987.
2. J. Delery and J. G. Marvin, *Turbulent Shock Wave Boundary Layer Interaction.* AGARDograph 280, 1985.
3. A. Jameson and D. A. Caughey, *A Finite Volume Method for Transonic Potential Flow Calculations.* AIAA 77-635, 1977.
4. J. D. McLean and J. L. Randall, *Computer Program To Calculate Three-Dimensional Boundary Layer Flows Over Wings With Wall Mass Transfer.* NASA CR-3123, 1978.
5. F. W. Steinle, Jr. and E. R. Pejack, *Toward an Improved Transonic Wind-Tunnel-Wall Geometry—A Numerical Study.* AIAA Paper 80-0442, March 1980.
6. F. T. Johnson, *A General Method for the Analysis and Design of Arbitrary Configurations in Compressible Flow.* NASA CR-3079, 1980.
7. S. J. Boersen and A. Elsenaar, *Half-Model Tests in the NLR High Speed Wind Tunnel HST: Its Technique and Application.*
8. F. W. Steinle and E. Stanewsky, *Wind Tunnel Flow Quality and Data Accuracy Requirements.* AGARD-AR-184, November 1982.